1982

NASA/ASEE SUMMER FACULTY RESEARCH FELLOWSHIP PROGRAM

MARSHALL SPACE FLIGHT CENTER
THE UNIVERSITY OF ALABAMA

PLASMA IGNITION FOR LASER PROPULSION

Prepared By:	Raymond F. Askew
Academic Rank:	Professor
University and Department:	Auburn University Physics and Mechanical Engineering
NASA/MSFC: Laboratory Division Branch	Structures and Propulsion Propulsion Auxiliary Propulsion
MSFC Counterpart:	T. Dwayne McCay
Date:	September 21, 1982
Contract No.:	NGT01-002-099 (University of Alabama)

PLASMA IGNITION FOR LASER PROPULSION

By

Raymond F. Askew
Professor of Physics and
Mechanical Engineering
Auburn University
Auburn, Alabama

ABSTRACT

The concept of space propulsion, using a remote laser as the continuous energy source for the space vehicle, requires a reliable mechanism to remotely initiate a plasma aboard the space vehicle. It has been suggested that this could be done using a pulsed power laser, properly focused within an onboard combustion chamber.

For a specific optical system a pulsed carbon dioxide laser having an energy output of up to 15 joules has been used to initiate a plasma in air at one atmosphere pressure. The spatial and temporal development of the plasma have been measured using a multiframe image converter camera. In addition the time dependent velocity of the laser supported plasma front which moves opposite to the direction of the laser pulse has been measured in order to characterize the type of wavefront developed.

Reliable and reproducible spark initiation has been achieved. The lifetime of the highly dense plasma at the initial focal spot has been determined to be less than 100 nanoseconds. The plasma front propagates toward the laser at a variable speed ranging from zero to 1.6×10^6 m/sec. The plasma front propagates for a total distance of approximately five centimeters for the energy and laser pulse shape employed.

ACKNOWLEDGEMENTS

Appreciation is expressed to the National Aeronautics and Space Administration for its support through the Research Fellows program. The cooperation and support of all NASA personnel in providing a challenging professional opportunity and environment in which to develop were outstanding. I am particularly in debt to Dr. Dwayne McCay for his continued words of encouragement and collaboration. To David VanZandt, my sincere thanks for his respect, understanding, and patience. And to Charles Smith, my admiration and gratitude for the type of professional and technical support every scientist always dreams of but never expects to receive. I thank you all.

LIST OF FIGURES

INTRODUCTION

The placement of satellites into geosynchronous orbit is presently accomplished by direct launch from the earth's surface. The need for such satellites for both commercial communication and defense purposes increases yearly. The space shuttle program provides a mechanism to transport such satellites to a space station at low earth orbit which can be used as a staging area for launching satellites into geosynchronous orbit. Current technology would utilize chemical propulsion for this secondary transfer in order to get the satellite into final orbit within a reasonable time after launch from the platform. This method requires a high fuel-to-pay load mass ratio. Alternative propulsion concepts to the above are needed to accomplish this interorbit transfer. Several have been suggested, among these being a process known as laser propulsion, as described by Kantrowitz(1). This process is shown diagramatically in Figure 1. A space station power laser system is directed to a rocket which is to transport the satellite to geosynchronous orbit. The on-board fuel is ignited by the focused laser beam and maintained as a plasma within a small volume of the engine. This plasma then transfers energy to the remaining fuel as it flows around the plasma core. The heated gas then exits through the expansion nozzle of the rocket engine thus providing thrust. A system based on this process is most attractive due to the high payload-to-total mass ratio which would be achieved.

It is well known that a focused laser can be used to create a small volume plasma in a gas(2),(3). However, the plasma so formed has been reported to immediately move toward the laser source(4),(5). This plasma motion results in the plasma front moving away from the focal volume of the laser beam, thus reducing the beam intensity on the plasma surface. This motion has been measured under limited conditions and theories have been proposed to explain its cause and the dynamics of the motion(6). Vastly improved time resolved experimental measurements of the early time plasma are needed, along with a better theoretical model of the laser beam-plasma interaction.

OBJECTIVES

The work reported here had as its original objective a broad detailed study of the behavior of the plasma formed by a focused pulsed laser. This included studies of several gases at various pressures using variable laser powers and pulse shapes. Due to time and equipment limitations only preliminary results could be achieved. The effort centered on studying the spatial and temporal behavior of the plasma formed in air at one atmosphere. This included a detailed analysis of the shape and size of the plasma formed and the speed of the plasma front as it moved toward the laser source. The primary intent was to develop an operational system which could achieve the broad objectives envisioned and to demonstrate its reliability while at the same time determining to what degree reproducible results could be obtained.

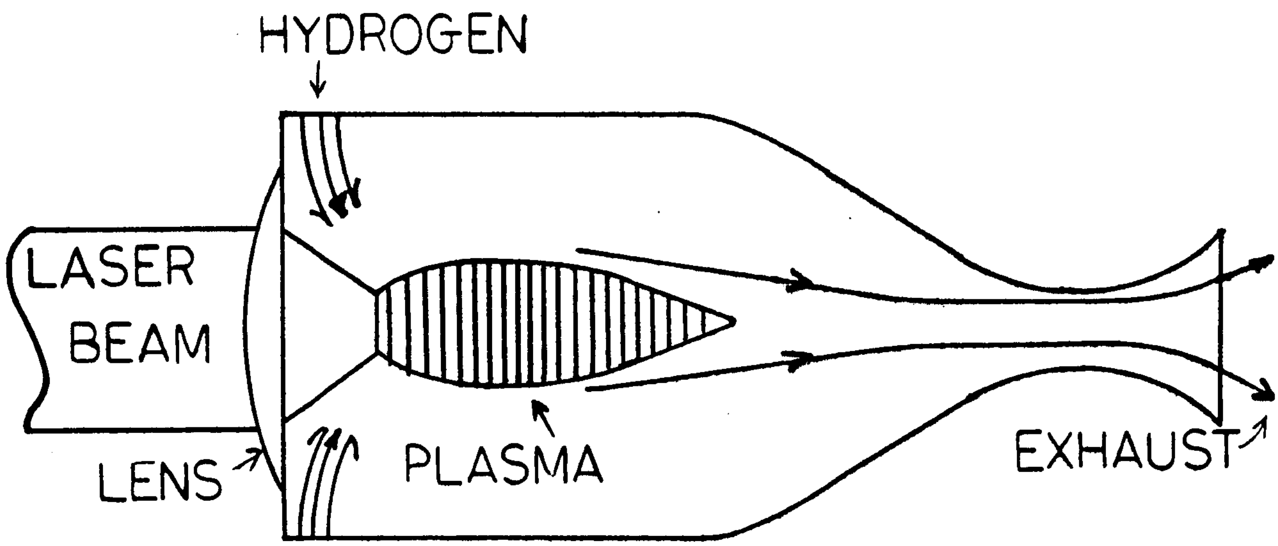

Figure 1. Laser Propulsion System.

EXPERIMENTAL ARRANGEMENT

Apparatus for conducting the experiment was assembled in such a manner as to be compatible with future experiments already planned. A block diagram of the experiment is shown in Figure 2. A Lumonics Model 103 TEA carbon dioxide pulsed laser was used as the energy source. It was modified to perform at approximately the following levels: 15 joules of energy in a pulse having a risetime of 40 nanoseconds, at a peak power of 5×10^7 watts, and with a primary pulse duration of 100 nanoseconds. The pulse had a small second peak with an exponential tail giving a total pulse duration of approximately 400 nanoseconds. The beam had a divergence of 0.6 milliradian half-angle. Time-dependent power measurement devices were not available to the experiment at the time of the studies reported here but will be in place for future measurements.

The turning mirror was front-surface gold-coated flat copper. The lens was NaCl having a focal length of 12 inches. The plasma was created within the enclosed chamber shown and all optical data were acquired through 2 inch diameter, 0.250 inch thick quartz flats. The system was optically aligned using a beam-splitter and a He-Ne laser.

The only diagnostic utilized was a TRW Model 1D1 image converter camera. Framing photographs were taken using Models 4B and 6B plug-in units. Streak photographs utilized Models 5B and 7B units.

The laser system was operated at 40 KV. When the storage capacitors were charged to this potential a trigger pulse was transmitted to a nitrogen filled spark gap. The subsequent breakdown of this gap initiated the current pulse to form the laser discharge.

The trigger pulse to the laser was also used to initiate operation of the image converter system. The system had a variable delay for opening the electronic camera shutter which could be varied from zero to 100 microseconds in increments of 10 nanoseconds. Due to the inherent delay of the laser system, particularly the spark gap, it was necessary to establish the true time delay to the camera shutter to insure that the camera recorded the initiation of the plasma formation. Careful cleaning of the spark gap resulted in a spark gap jitter which was generally less than 20 nanoseconds, with an upper limit of less than 100 nanoseconds. For the system as operated at full laser potential, the delay to the camera from the delay unit was nominally 2.21 to 2.23 microseconds for the streak units and 2.18 to 2.19 microseconds for the framing units.

The image converter camera used a 40 cm focal length, f/5.6 lens to collect light for the image tube. Events were recorded using Polaroid Type 57 (ASA 3000) film.

Alignment of the unfocused beam and evaluation of the beam pattern were performed each day, prior to insertion of the lens, using a thermally sensitive plastic film at the position of the alignment beam splitter, at the mirror position, and at the top of the test chamber. A normal beam pattern is shown in Figure 3.

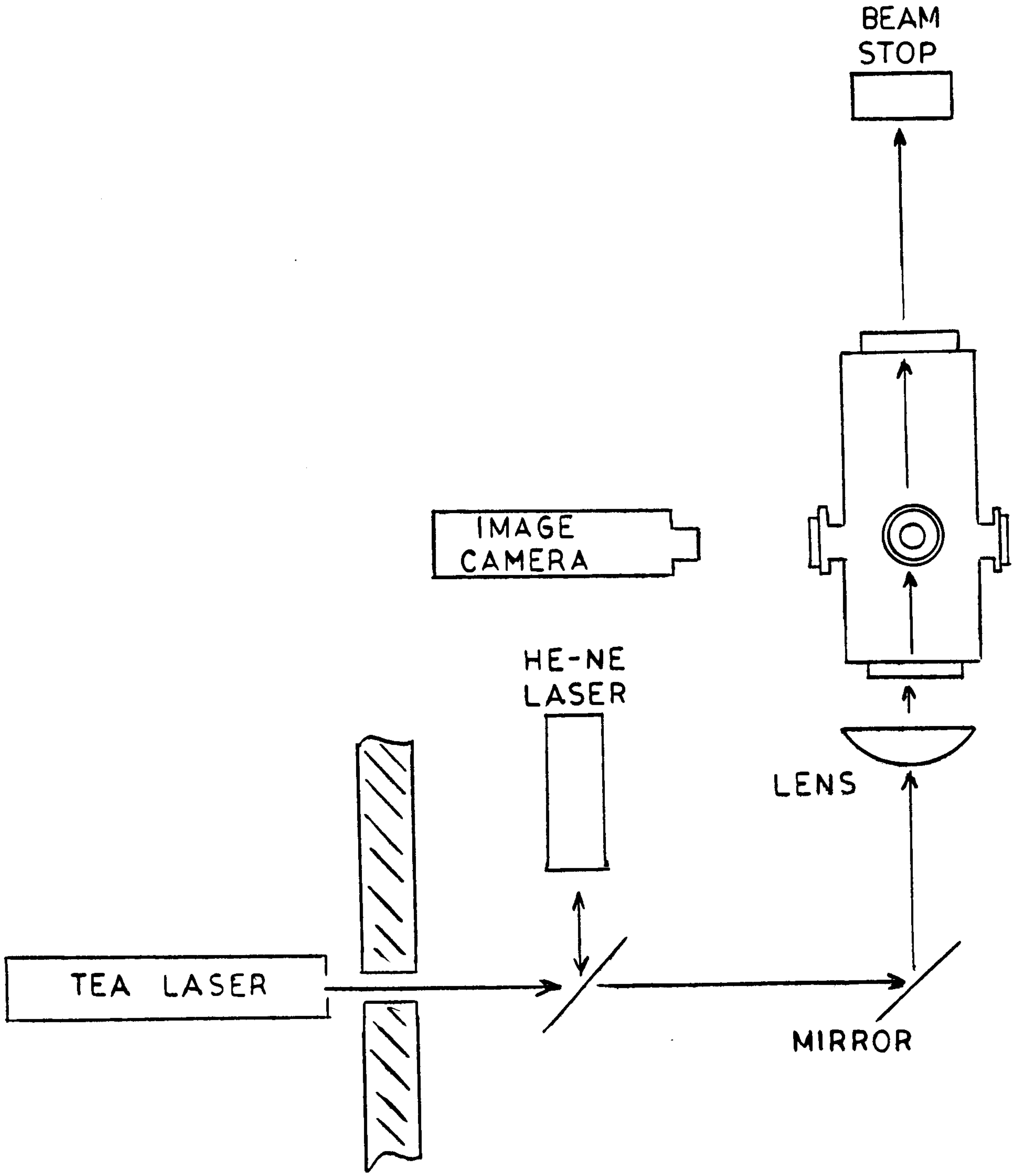

Figure 2. Experimental Arrangement.

Optical magnification of the recording system was accomplished by photographing a precision grid placed in the center of the test chamber and viewed through the quartz window.

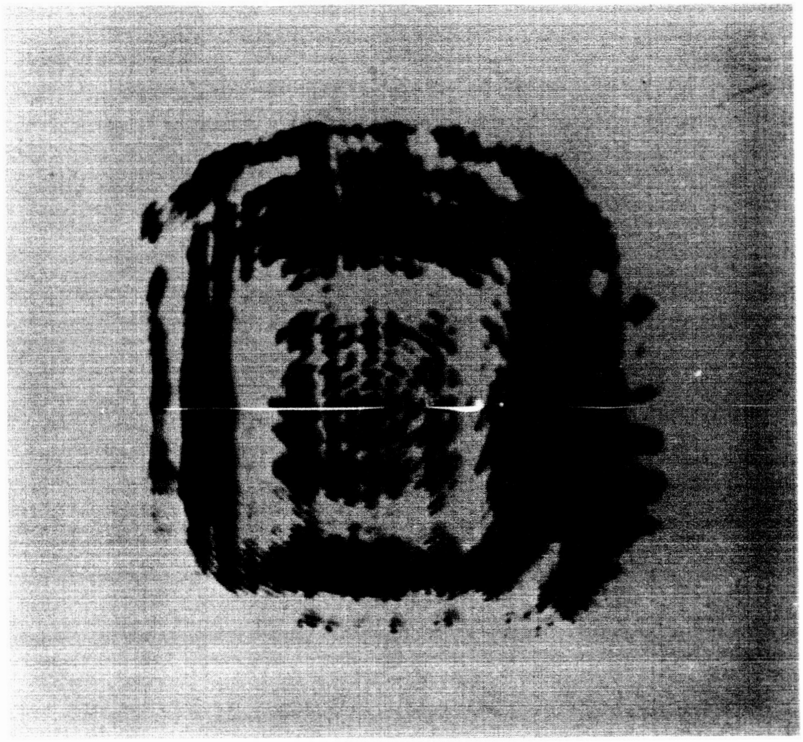

Figure 3. Laser Burn Pattern

Streak and framing times, as well as interframe delays of the image converter system, were carefully measured using a high speed storage oscilloscope. This provided accurate calibration of the time of events and of the streak time on the film.

RESULTS

Figure 4 shows two sets of framing exposures of a laser produced plasma, produced under essentially the same conditions. The time of exposure for each frame is 200 nanoseconds (ns) for set (a) and 100 ns for set (b). The interframe delay in each case was 0.5 microsecond (μs). The first event recorded is at the bottom of each picture, with later events at the top. For orientation, the laser beam was directed from the bottom of the picture toward the top. For scale reference, the length of the plasma shown in (b) is 5 millimeters (mm) in the first frame, 6 mm in the second, and 7 mm in the third. The considerable difference in the detail between the two events as recorded is due to exposure time. The longer exposure (200 ns) results in loss of development detail.

Figure 5 shows six different events, each with multiple frames. The exposure time was 50 ns. The initiation of image recording was prior to the initiation of the plasma in the first set (a). The first frame is therefore blank. The second frame (first image) thus occurred no more than 0.5 μs after plasma ignition. The considerable plasma shown indicates a very rapidly developing system. The second set of events (b) appears to have begun late in time since the first frame of each is very well developed. For scale reference, the length of the plasma of the first frame of the third event in (b) (lower right corner) is 1.9 cm.

Two observations concerning these photos are appropriate. First, due to the limited aperture of the camera, when the plasma extended below the camera viewing region there was a cutoff of the image. This has occurred in the third frame of all six events of Figure 5. The somewhat flat lower end of each frame is the result of such a cutoff. Secondly, the bright horizontal lines which appear in some frames throughout these data are an effect due to the camera. This occurs at specific geometric locations on the camera screen when the light intensity onto the photocathode exceeds a prescribed limit in those areas.

To obtain better information on the details of development of the plasma, the preceeding figures indicate the need for shorter exposures and shorter interframe delays. Figure 6 shows the three frame development of ten events, each having 20 ns exposures. Of special note is the first frame of the third event of (a) (bottom right corner). This event has been recorded very early in time. Since only 50 ns separate the second frame from the first, if one includes the 20 ns exposure of frame 2, the maximum time for the plasma length difference as shown in the first two frames would be 70 ns. The lengths of these two images are 6.6 mm and 13.2 mm respectively. Thus the average speed of the plasma front is 9.4×10^4 m/s. The long faint streak which appears to join the second and third frame images in (a) and (b) is due to using an interframe delay which was not at least four times the exposure time.

Figure 7 shows four events using 5 ns exposures. Considerable detail can be seen in these which would indicate the formation of several distinct events along the plasma length, each changing rapidly in time.

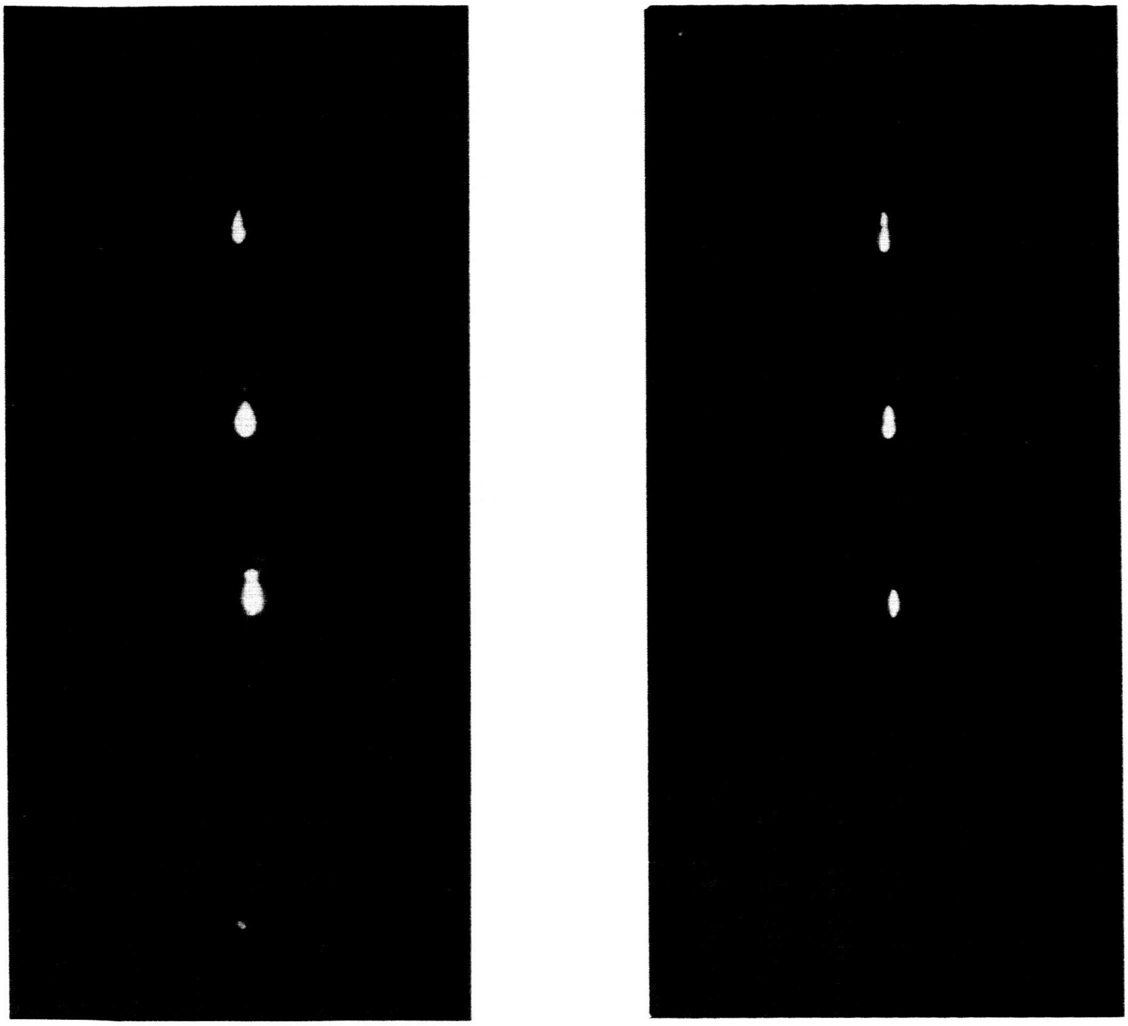

(a) (b)

Figure 4. Multiple Frame Photographs of Laser Produced Plasmas. Air at 1 Atmosphere Pressure.

(a) Exposure: 200 ns; Interframe Delay: 0.5 μs
(b) Exposure: 100 ns; Interframe Delay: 0.5 μs

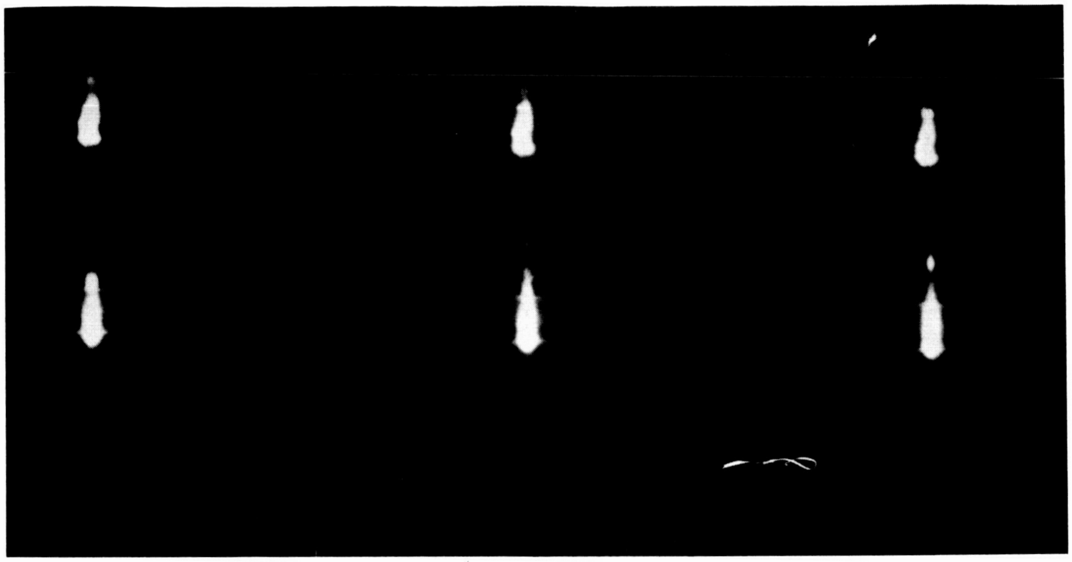

(a)

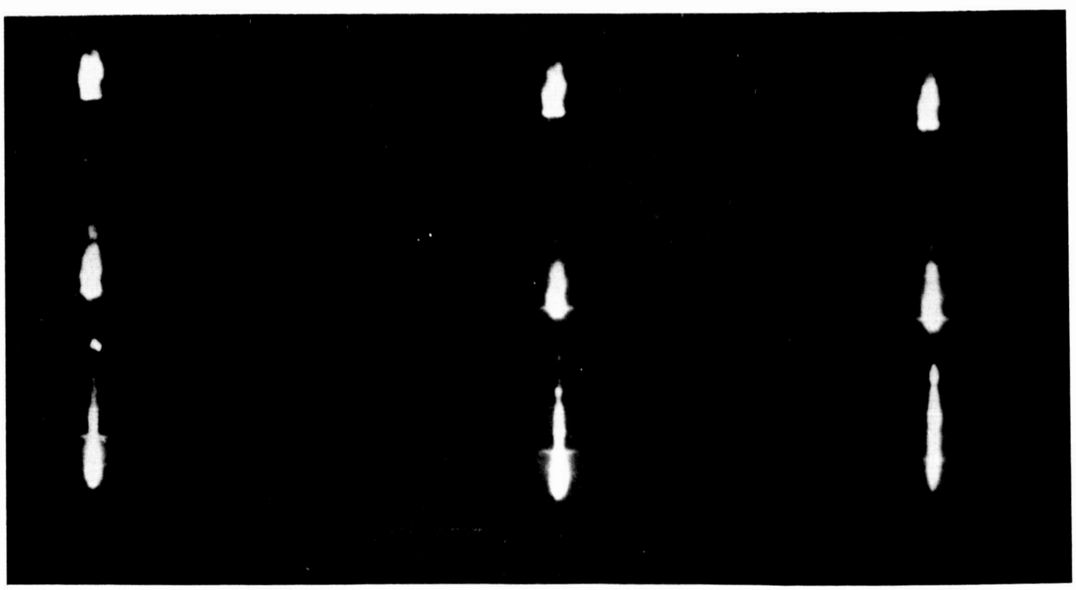

(b)

Figure 5. Multiple Frame Photographs of Laser Produced Plasmas. Air at 1 Atmosphere Pressure.

Exposure: 50 ns Interframe Delay: 0.5 μs

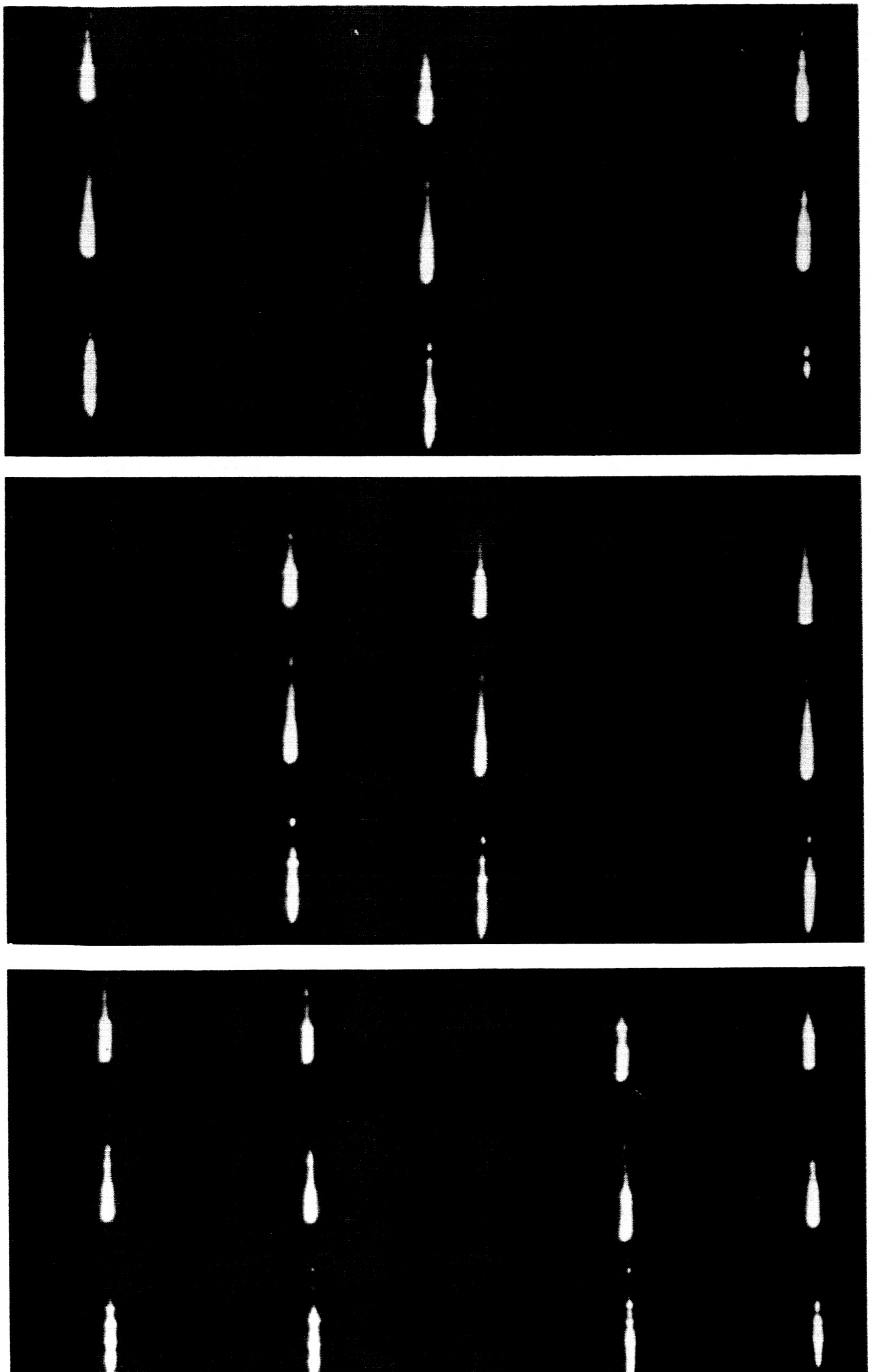

(a)

(b)

(c)

Figure 6. Multiple Frame Photographs of Laser Produced Plasmas. Air at 1 Atmosphere Pressure.

Exposure: 20 ns Interframe Delay: 50 ns

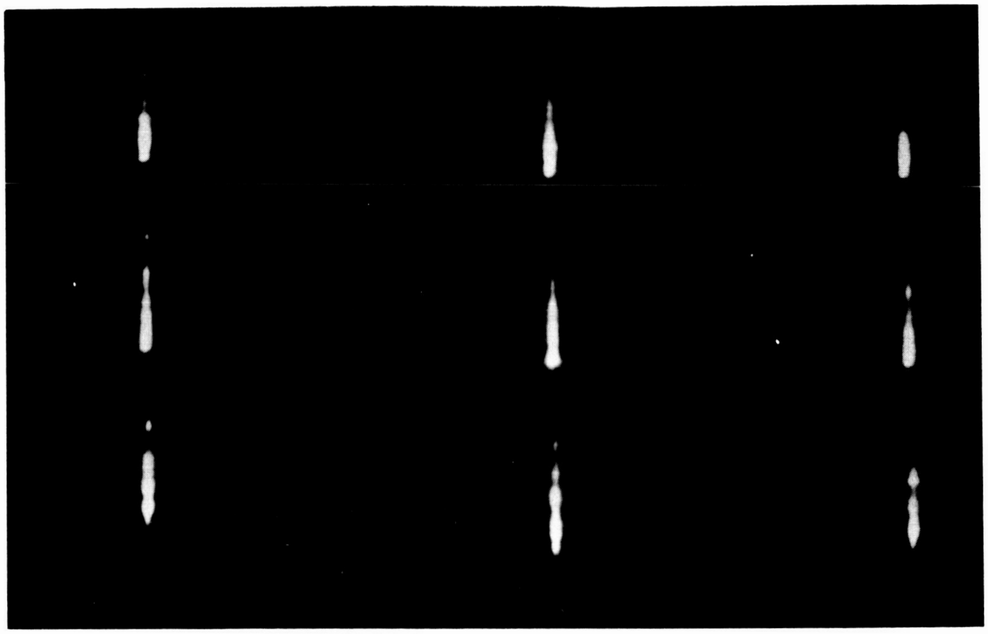

(a)

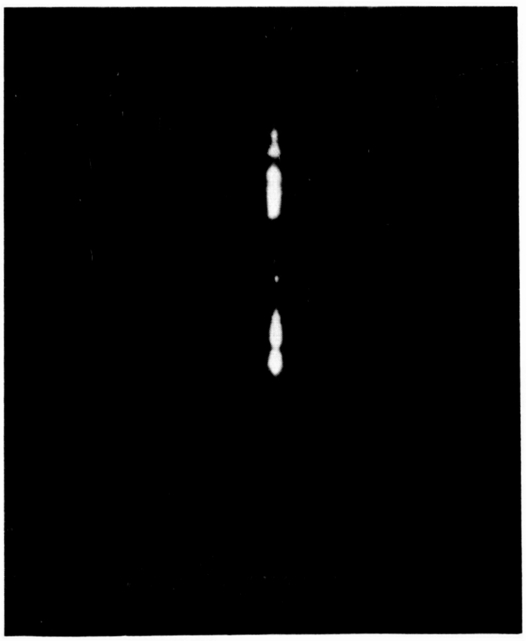

(b)

Figure 7. Multiple Frame Photographs of Laser Produced Plasmas. Air at 1 Atmosphere Pressure.

Exposure: 5 ns Interframe Delay: 50 ns

Figure 8 shows three events having 20 ns exposures at 100 ns interframe delays. These events have been photographed after turning the image through a 90° rotation. The first frame is at the bottom of the picture, the third at the top. The laser source is located to the left and propagates left-to-right. The first frame on the lower left shows an initiation spot to the right extreme with a large separation to a second spot from which the plasma appears to spread irregularly to the left (toward the laser source). The total length of this event is approximately 1.9 cm. Note that the camera aperture terminates the image on the left side for every frame shown in this figure.

Figures 9 & 10 show frames (one to three) for thirteen events using an exposure of 10 ns with an interframe delay of 50 ns. The first frame of the first event (a) in Figure 9 is an extremely early stage development photograph. Noting that the second frame already extends beyond the aperture edge, we can calculate from the expansion of the second spot the average speed of the plasma front. The maximum time between frames would be 60 ns. The total length of the plasma, from first spot to the left edge in frame two is 1.7 cm. The second spot has extended at least 1.4 cm in this time. Thus the average speed must exceed 2.3×10^5 m/s. The remaining events in Figures 9 & 10 show various stages of plasma development. All events have a great deal in common in that each appears to have an initial plasma which is disconnected visually from the following plasma. Considerable structure continues to appear in early time.

Where the initial spot is clear in framing photos, its size appears to never be larger than one millimeter. At times it appears as small as 0.5 mm. The wide plasma glow which appears to move back toward the laser grows to a width of approximately 2 mm in the early times (100 - 150 ns). For the optical geometry chosen the convergence cone of the laser beam after passing through the lens had a half angle of approximately 7°. For the frames shown in Figures 9 & 10, the divergence angle toward the laser source beginning at the initial plasma spot is between 3° and 5° half angle.

Figure 11 shows several very typical streak photographs of the early time plasma formation. All were taken using a total streak time of 200 ns, although each plasma is initiated at a different time following the initiation of the streak. Because of a vertical offset in the image converter orientation, there is an offset to the zero velocity slope on all streak photographs. This has been corrected for in the calculations which were performed to yield velocities.

One can see, particularly in (b) & (c), what appear to be high speed ejections from the already formed plasma front. These ejections, particularly the early time ones, reach speeds of 1.6×10^6 m/s. The speed of the radiating front shows large scale changes several times for each event.

Figures 12 and 13 show streak photographs of fourteen events, all having a 200 ns streak time. The general similarity of all streaks at 200 ns times is excellent. The velocities measured from these images are quite reproducible. The late time velocity approaches 10^4 m/s in all afterglows.

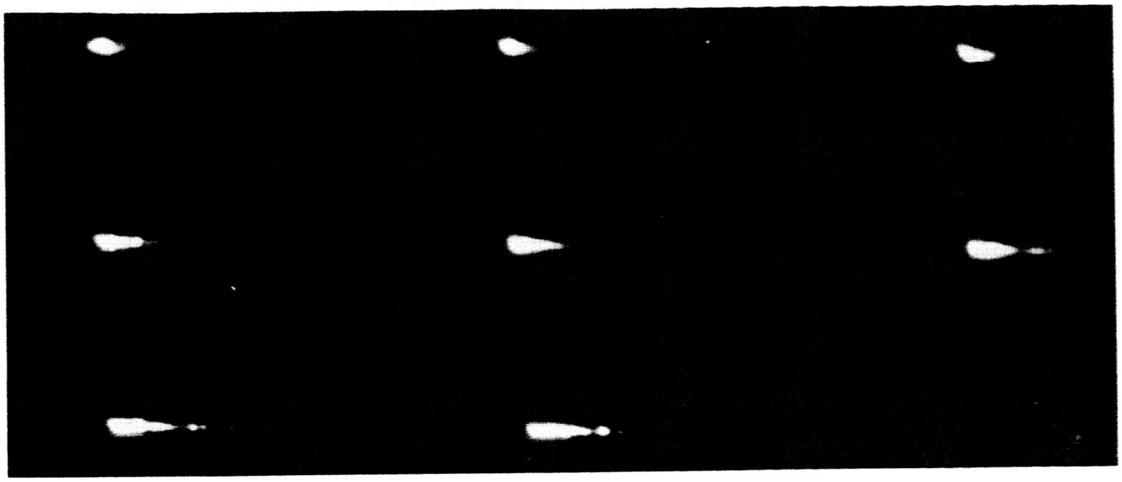

Figure 8. Multiple Frame Photographs of Laser Produced Plasmas. Air at 1 Atmosphere Pressure.

Exposure: 20 ns   Interframe Delay: 100 ns

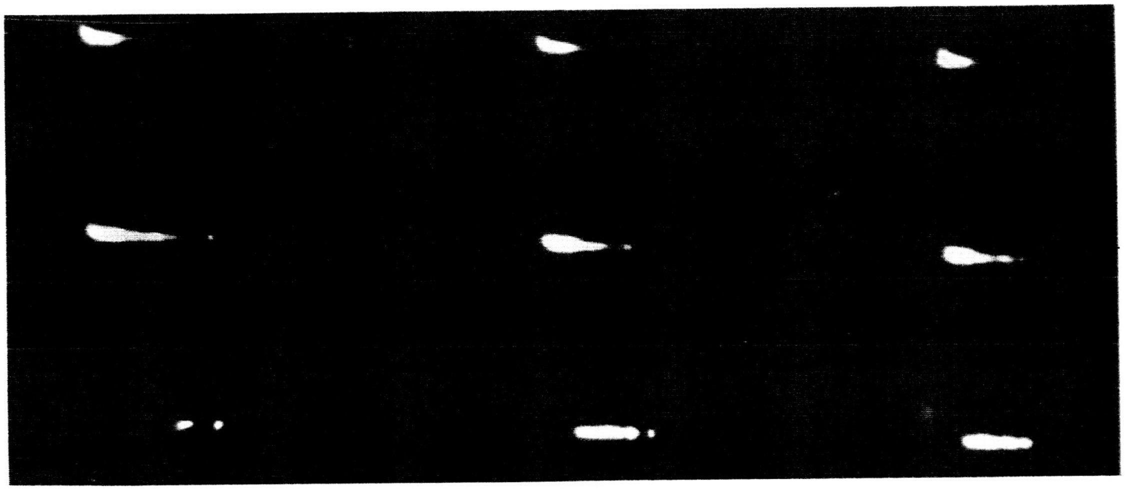

(a)

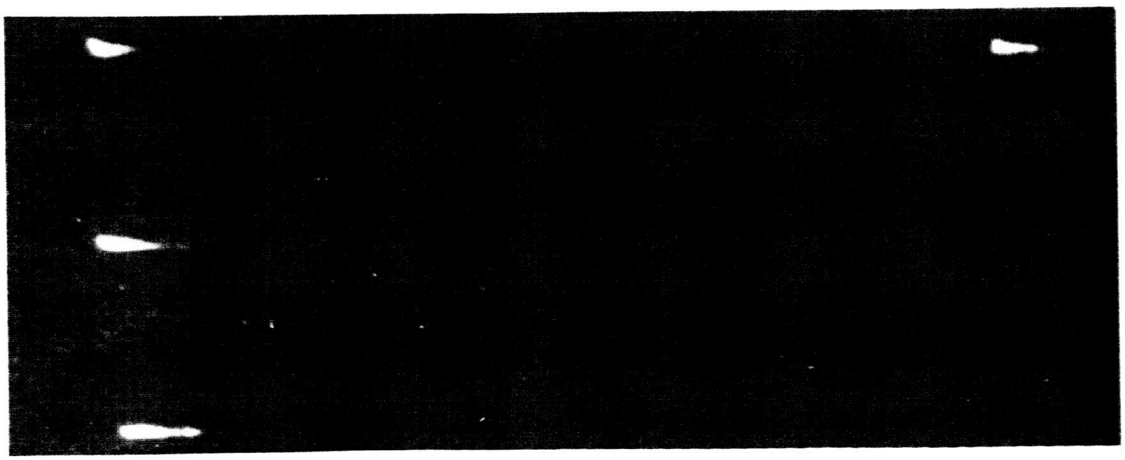

(b)

Figure 9. Multiple Frame Photographs of Laser Produced Plasmas. Air at 1 Atmosphere Pressure.

Exposure: 10 ns   Interframe Delay: 50 ns

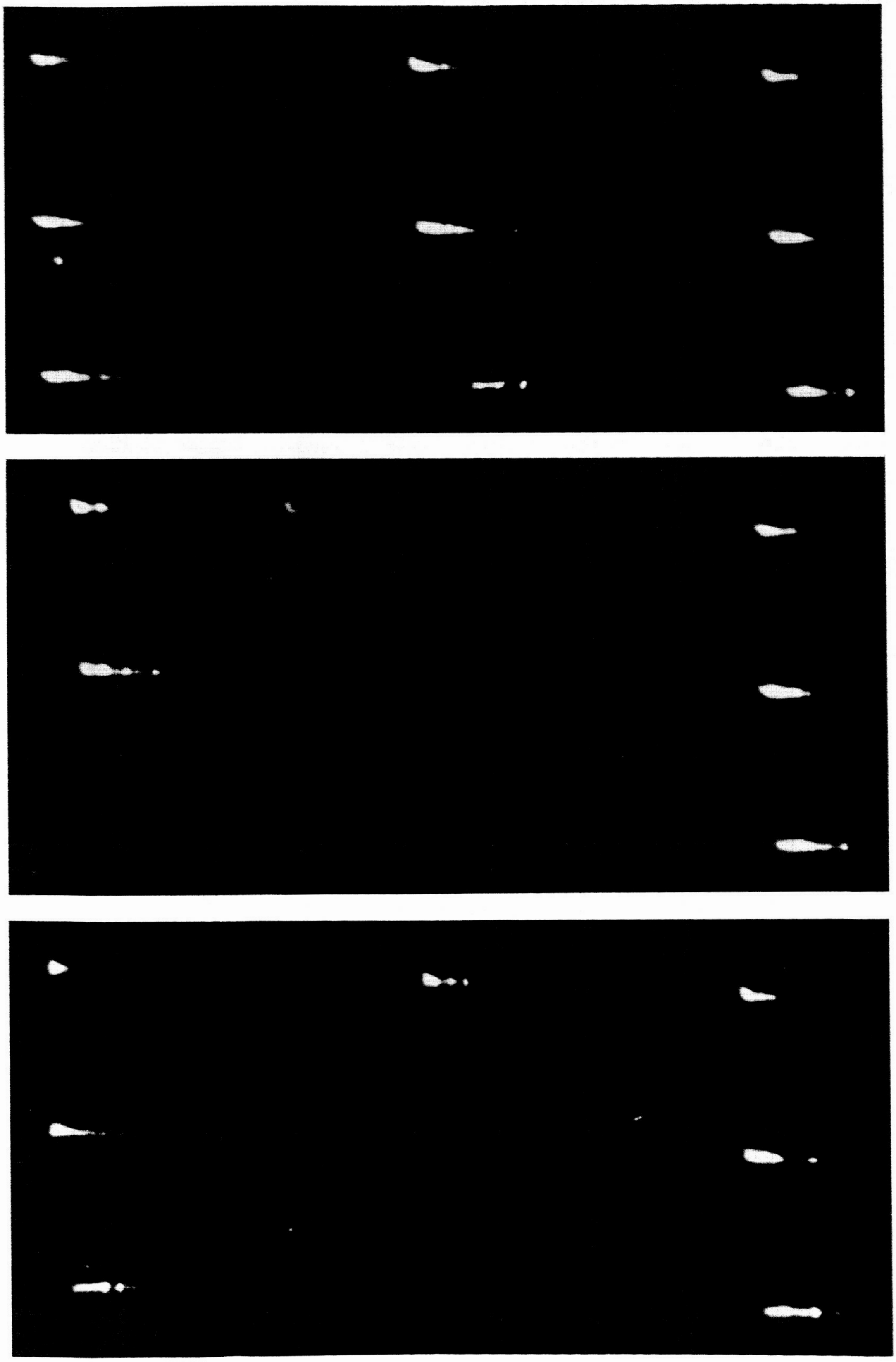

(a)

(b)

(c)

Figure 10. Multiple Frame Photographs of Laser Produced Plasmas. Air at 1 Atmosphere Pressure.

Exposure: 10 ns Interframe Delay: 50 ns

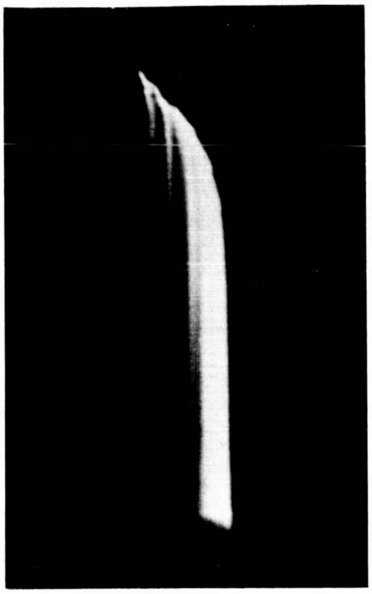

(a)

(b)

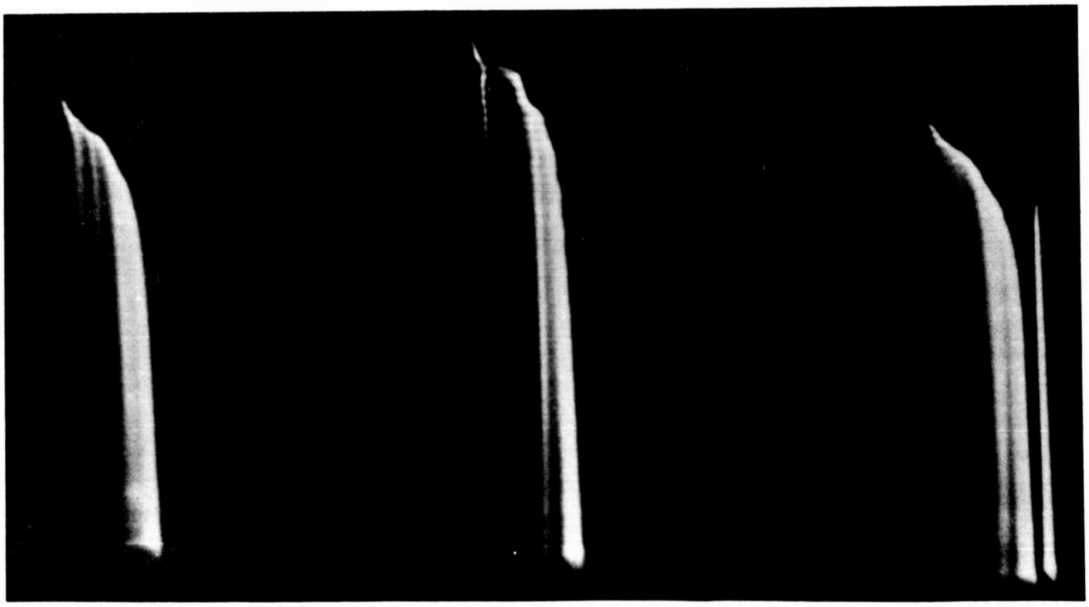

(c)

Figure 11. Streak Photographs of Laser Produced Plasmas. Streak Duration: 200 ns. Air at 1 Atmosphere Pressure.

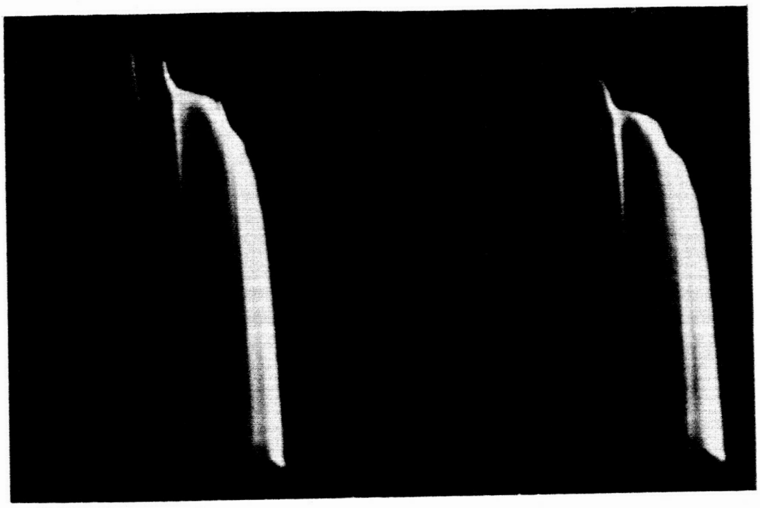

(a)

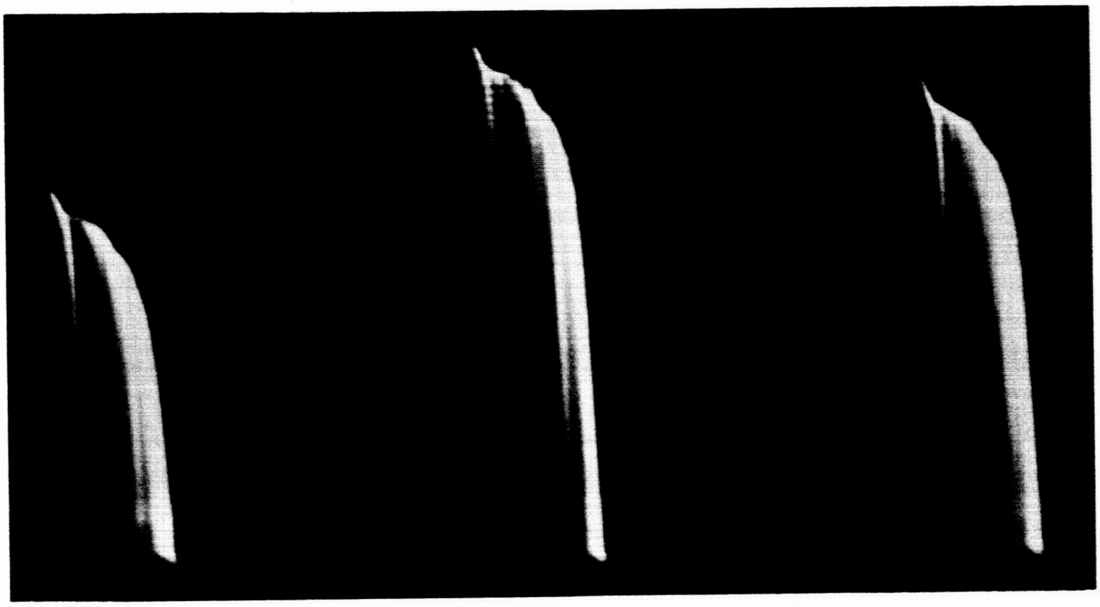

(b)

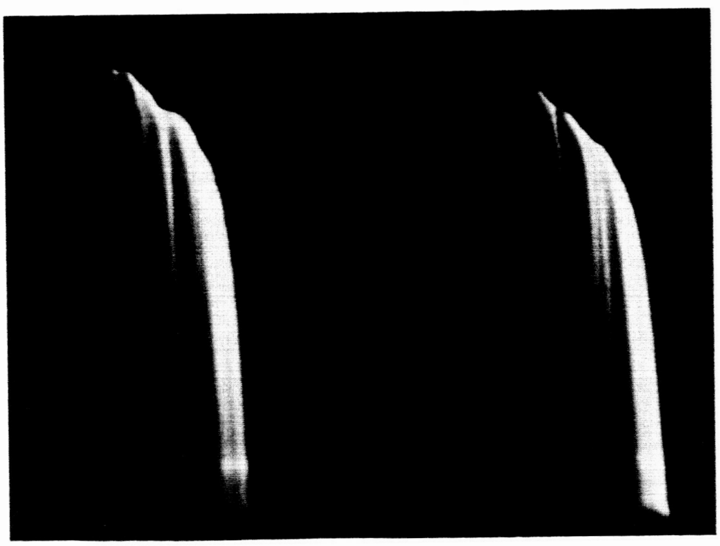

(c)

Figure 12. Streak Photographs of Laser Produced Plasmas. Streak Duration: 200 ns. Air at 1 Atmosphere Pressure.

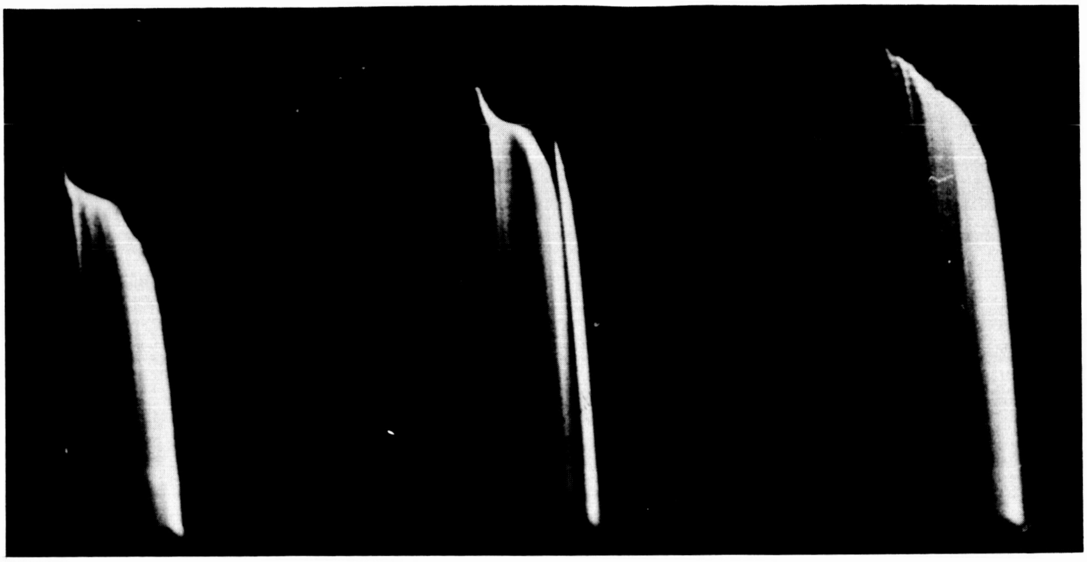

(a)

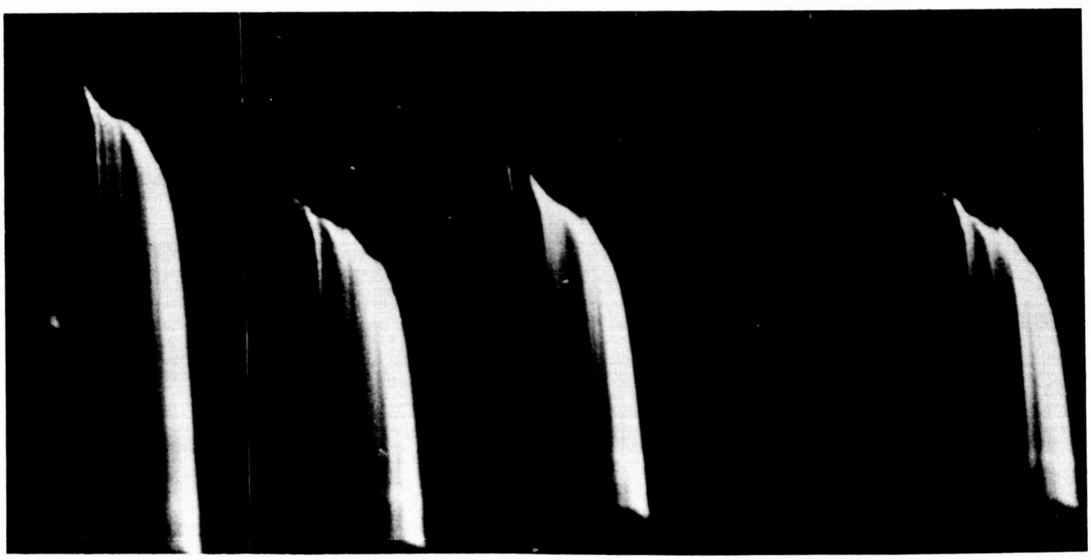

(b)

Figure 13. Streak Photographs of Laser Produced Plasmas. Streak Duration: 200 ns. Air at 1 Atmosphere Pressure.

Figures 14 & 15 show thirteen events at streak times of 100 ns. These appear to be two types of structures. One has high speed ejections connecting each portion of the plasma, such as is seen in Figure 14 (a) & (b). Others as seen in Figure 15 show isolated points within the discharge.

To try and obtain better resolution of the streak behavior, streak photographs were taken at 50 ns exposures. These are shown in Figure 16. As can be seen from these images there is considerable structure to the early time plasma. Several separate plasma sources are generated without any apparent physical coupling. The mechanisms involved in the generation of these separate plasmas are not understood at this time.

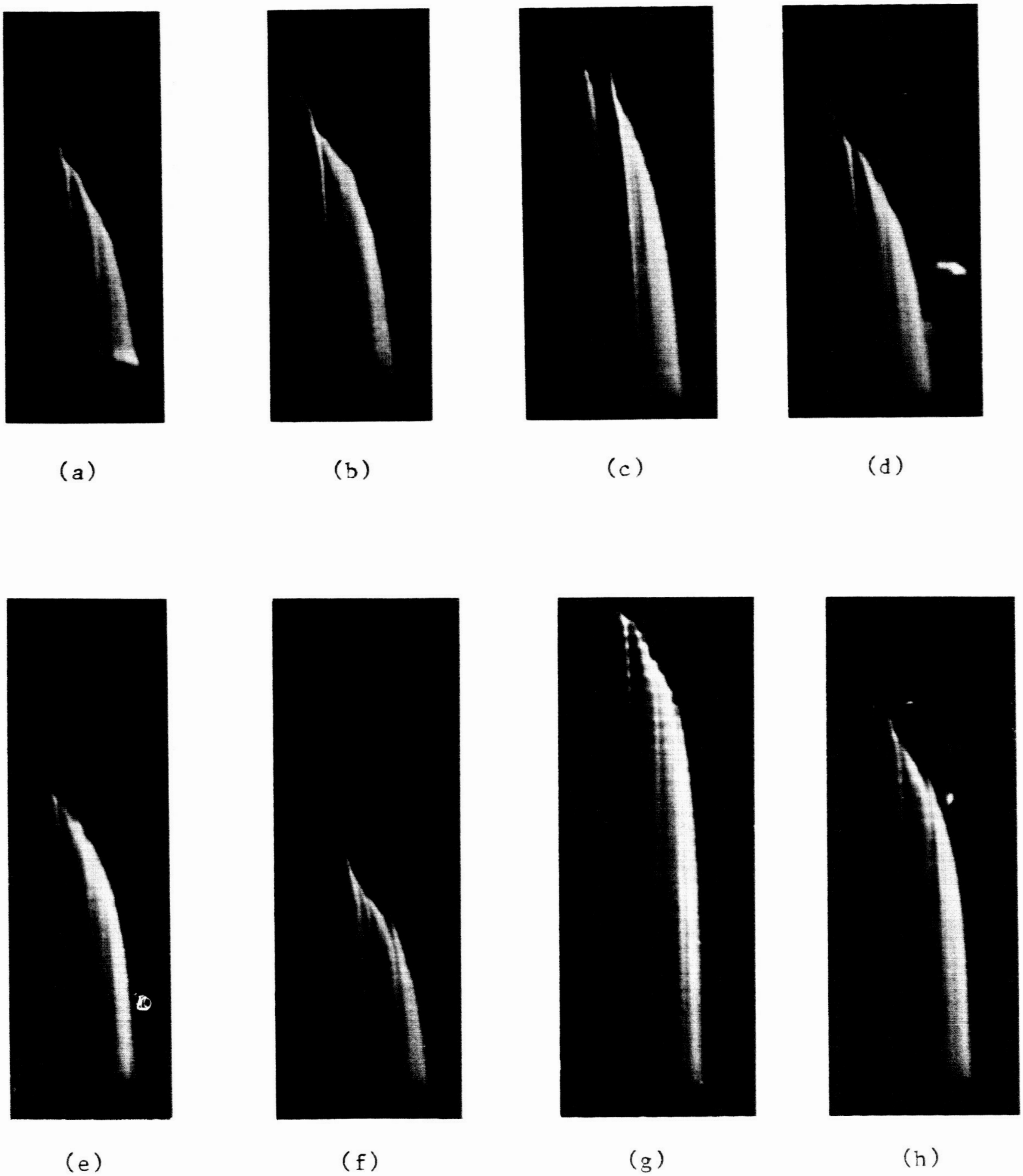

Figure 14. Streak Photographs of Laser Produced Plasmas. Streak Duration: 100 ns. Air at 1 Atmosphere Pressure.

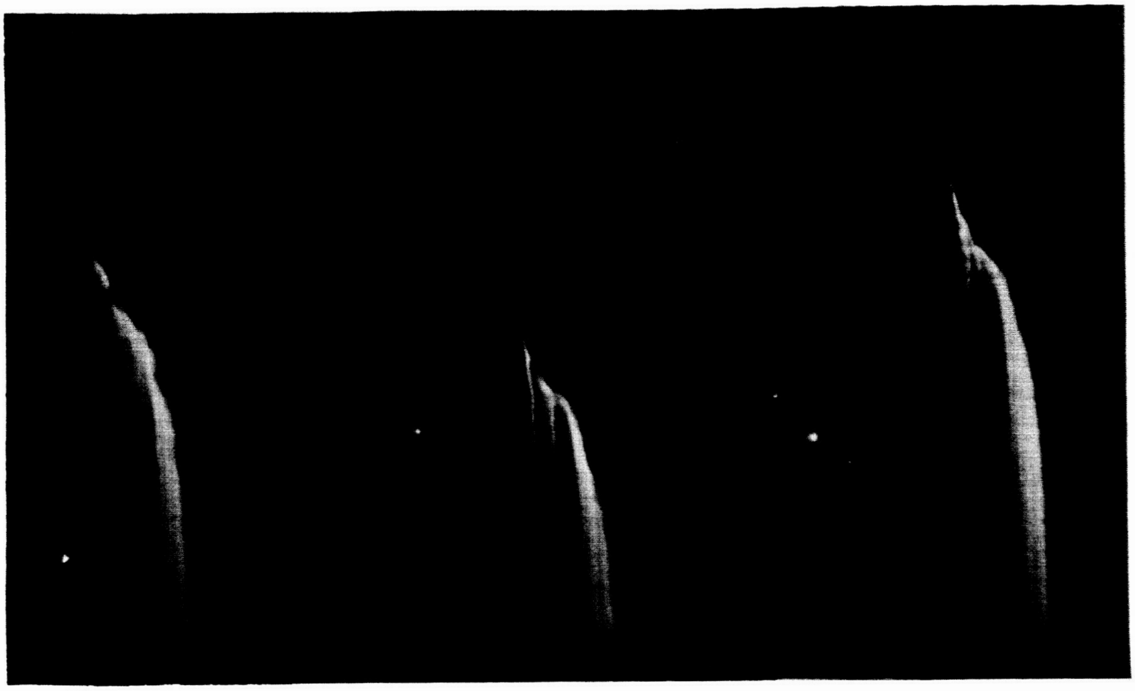

(a)

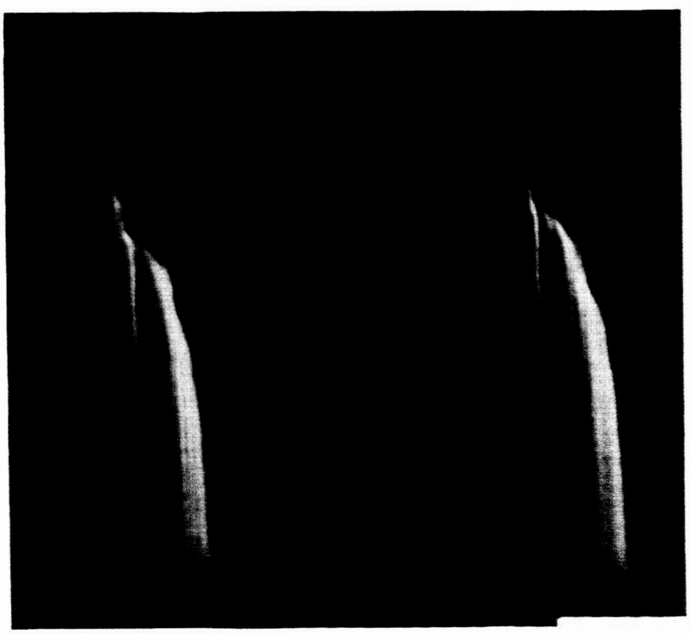

(b)

Figure 15. Streak Photographs of Laser Produced Plasmas. Streak Duration: 100 ns. Air at 1 Atmosphere Pressure.

(a)

(b)

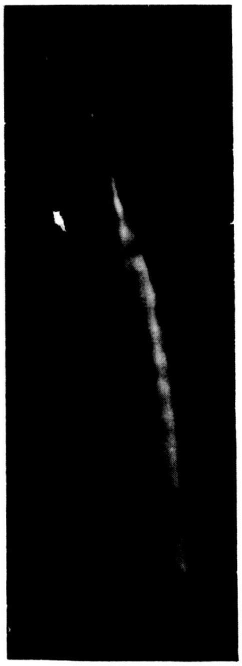

(c)

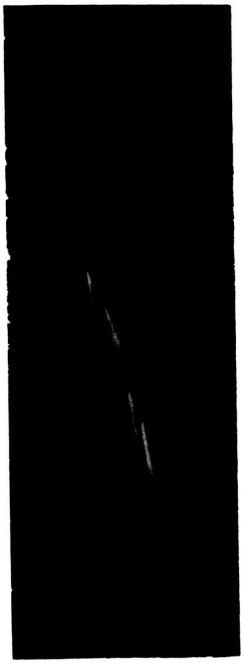

(d)

Figure 16. Streak Photographs of Laser Produced Plasmas. Streak Duration: 50 ns. Air at 1 Atmosphere Pressure.

CONCLUSIONS & RECOMMENDATIONS

The apparatus to test and investigate initial spark breakdown phenomena has been assembled and tested. The system has been successfully operated to demonstrate the ability to produce breakdown in air at a predetermined location and to synchronize this event with a high speed image framing and streak camera for both types of operations.

Photographs obtained demonstrate a high degree of reproducibility for plasmas produced by focused laser radiation. The infrastructure of such plasmas has a number of "hot spots" that appear at different points in time following the creation of the first plasma. Earlier image photographs of a plasma similarly produced were reported by Pigott(7). There is little similarly between the photographs shown here and those of Pigott. The isolated initial spot appears in many of Pigott's photographs. All of his photographs, however, are taken at least one microsecond after plasma initiation. All early time detail has thus been lost.

Streak photographs indicate the presence of high speed ejections from a relatively slow moving front. These ejections are toward the laser source and have speeds up to 1.6×10^6 m/s, whereas the usual speed of propagation of the radiative front is much slower. This value is considerably higher than that reported by Raizer and Kozlov of 1×10^5 m/s. The initial plasma spot never shows a speed in excess of 1×10^4 m/s. Each high speed ejection rapidly (usually in less than 5 ns) slows, soon reaching a somewhat uniform propagation speed of the order of 10^4 m/s. Although we do not observe the total length of the discharge due to aperture cutoff it would appear that the speeds for the plasma front as measured late in time would continue to slow as uniformly as is shown in the streak photographs. This would result in a lifetime for the radiating plasma of the order of 5 μs, with the plasma having a total length of approximately 5 cm. These numbers are consistent with separate time lapsed photography used to determine the total length, and framing and streak photographs having durations in excess 5 μs.

Because it was not possible to measure the power levels and energy input to the air, results are only qualitative. To be able to model the phenomena occurring in this plasma, a measure of the energy input as a function of time is necessary. Equipment currently on order will allow for this to be done once in place. In addition, a new chamber facility will be constructed which will allow a view of the entire length of the plasma.

With the new facility and energy measuring equipment the originally conceived program of study over a range of pressures and power levels can be carried out. Because of the consistent shape of the plasma cone produced and the closeness of the cone angle of the converging laser beam to the diverging plasma cone, experiments using lenses of different focal lengths would be desirable.

REFERENCES

1. A. R. Kantrowitz, J. of Astronautics and Aeronautics, 9, 34 (1971).

2. D. C. Smith, J. App. Phys., 41, 4501 (1970).

3. N. A. Generalov, V. P. Zimakov, V. A. Masyukov, and Yu. P. Raizer, Sov. Phys. JETP Lett. 11, 228 (1970).

4. Yu. P. Raizer, Sov. Phys. Usp. 23, 789 (1980).

5. G. I. Kozlov, Sov. Phys. Tech. Phys. 24, 37 (1979).

6. N. Kroll and K. M. Watson, Phys. Rev. A 5, 1883 (1972).

7. J. C. Pigott, AEDC-TR-71-35, March, 1971.